Anal. Bioanal. Electrochem., Vol. 16, No. 12, 2024, 1109-1121
https://www.doi.org/10.22034/abec.2024.719416

Analytical & Bioanalytical Electrochemistry

Full Paper

Synergistically Enhanced Electrocatalytic Performance of Mn-Co-Ni Oxides/rGO Composite for Efficient Oxygen and Hydrogen Evolution Reactions

Mehdi Mehrpooya,[1,2,*] and Seyed Sina Hosseini[1,2]

[1]*School of Energy Engineering and Sustainable Resources, College of Interdisciplinary Science and Technology, University of Tehran, Tehran, Iran*
[2]*Hydrogen and Fuel Cell Laboratory, University of Tehran, Tehran, Iran*

*Corresponding Author, Tel.: +98(21)88497167
E-Mail: mehrpoya@ut.ac.ir

Received: 5 November 2024 / Received in revised form: 19 December 2024 / Accepted: 24 December 2024 / Published online: 31 December 2024

Abstract- This study presents the development of a highly efficient NiCoMn@N,Co-rGO electrocatalyst designed to facilitate electrochemical water electrolysis, specifically addressing both the Oxygen Evolution and Hydrogen Evolution Reactions. This catalyst features a novel hybrid nanostructure comprising Co-Ni-Mn oxides integrated onto nitrogen- and cobalt-co-doped reduced graphene oxide (N,Co-rGO). The synthesis involved the improved Hummers' method for graphene oxide preparation, followed by nitrogen and cobalt doping via calcination, and deposition of Co-Ni-Mn oxides through a solvothermal process. Physicochemical and electrochemical characterizations confirmed the successful formation of a mesoporous structure and efficient synergy between the metal oxides and graphene substrate. The NiCoMn@N,Co-rGO composite exhibits superior catalytic efficiency in facilitating the Oxygen Evolution Reaction in alkaline media, achieving a potential of 1.58 V at 10 mA/cm² (overpotential: 0.27 V), compared to 1.62 V (overpotential: 0.50 V) for NiCoMn oxide. For the Hydrogen Evolution Reaction, it achieves a potential of -0.50 V at -10 mA/cm² (overpotential: 0.49 V), similar to NiCoMn oxide. The improved efficiency is ascribed to the synergistic effects of nitrogen and cobalt doping in the reduced graphene oxide framework, improving conductivity, active site accessibility, and structural stability. These findings establish NiCoMn@N,Co-rGO as a more efficient electrocatalyst for OER.

Keywords- Water electrolysis; Oxygen Evolution Reaction; Hydrogen evolution reaction; Electrocatalyst; Metal oxide; Graphene

1. INTRODUCTION

The excessive reliance on fossil fuels led to severe environmental challenges [1], such as increased greenhouse gas emissions, global warming, and shifts in climate patterns [2]. Furthermore, the diminishing reserves of fossil fuels highlight the urgency of transitioning to alternative, sustainable energy sources. In response to these challenges, significant research efforts have focused on developing sustainable and cost-effective energy technologies to meet the rising global energy demand while minimizing environmental impacts [3]. Hydrogen, distinguished by its environmentally friendly nature, zero emissions, and high energy density, is regarded as a highly promising energy carrier. Among various hydrogen production technologies, water electrolysis stands out, driven by fundamental electrochemical processes, including the hydrogen evolution reaction (HER) and the oxygen evolution reaction (OER) [4]. These reactions serve as the cathodic and anodic processes, respectively, in water electrolysis systems, playing a pivotal role in their operation. Water electrolysis, a widely adopted technique, enables the generation of hydrogen fuel from water, yielding hydrogen and oxygen as by-products [5].

Noble metal catalysts, such as Ir and Ru-based catalysts for the OER and Pt-based catalysts for the HER [6,7], are recognized for their outstanding catalytic activity. However, their high cost and limited availability pose significant barriers to large-scale commercial implementation [4]. To address this issue, extensive research has been directed toward the advancement of catalysts based on non-precious metals. For HER, metal alloys involving elements such as Ni, Mo, Co, Cu, and Cr, have shown significant potential through structural engineering and doping strategies, leading to high catalytic performance comparable to Pt [8]. Similarly, for OER, transition metal oxides and hydroxides, particularly those based on Fe, Co, and Ni, along with their oxides, hydroxides and nitrides, have emerged as cost-effective alternatives [9]. These advancements highlight the viability of non-noble metal catalysts in replacing precious metals like Ir and Ru, offering scalable and economically sustainable solutions for energy applications [10,11].

Specifically, transition metal oxides are promising alternatives to precious metals in case of HER and OER [12] due to their low cost and abundant availability, but they suffer from poor electrical conductivity, tendency to aggregate, and limited stability under harsh electrochemical conditions. In this context, two-dimensional carbon materials like graphene have come to the fore with unique properties, serving as a complementary component [13], alongside metal oxides to enhance catalytic performance in OER and HER, by providing uniform dispersion of metal oxide nanoparticles, and improving the structural integrity of the catalyst thereby overcoming the aforementioned weaknesses of bare metal oxide particles [14]. Moreover, the interaction between graphene and transition metal oxides often results in synergistic effects, such as charge redistribution and modulation of the electronic structure, which lower the energy barriers for HER and OER, thereby boosting catalytic activity. This combination of graphene's

unique properties with the intrinsic activity of transition metal oxides creates a highly efficient, durable, and cost-effective system for water splitting and other renewable energy applications [15].

To enhance the efficiency of hydrogen production via water electrolysis, the design of highly effective electrocatalysts for the oxygen evolution and hydrogen evolution reactions is critical. In this study, we utilized a composite structure comprising transition metal (Ni-Co-Mn) oxides embedded within a cobalt and nitrogen-doped reduced graphene matrix as a dual-functional catalyst for HER and OER. This unique hybrid structure combines the catalytic benefits of transition metal oxides with the excellent electrical conductivity and stability provided by the doped graphene support. Prior to this work, the catalytic performance of the composite was extensively investigated by the authors for the oxygen reduction reaction (ORR) [3], where it demonstrated superior activity. The synergistic effects between the metal oxides and the graphene framework were identified and confirmed, highlighting their combined contribution to enhanced catalytic performance. This work presents a novel application of the Ni-Co-Mn oxide composite embedded in a doped graphene matrix for water-splitting reactions (HER and OER), expanding its proven efficacy in ORR catalysis. The study not only demonstrates the versatility of this composite material but also sheds light on the underlying synergistic mechanisms driving its catalytic performance. This dual functionality holds great promise for promoting sustainable hydrogen production methods.

2. EXPERIMENTAL SECTION

2.1. Catalyst synthesis

In this study, a composite material consisting of Co-Ni-Mn oxides embedded within heteroatom-doped reduced graphene oxide (NiCoMn@N,Co-rGO), with atomic cobalt and nitrogen as dopants, was utilized and evaluated for its performance in water electrolysis. The detailed synthesis procedure has been described in our previous work [3]. Briefly, the fabrication involved three key steps: first, the preparation of cobalt- and nitrogen-doped reduced graphene oxide (N,Co-rGO); second, the synthesis of Co-Ni-Mn oxides; and finally, the integration of the synthesized oxides onto the N,Co-rGO substrate to form the final NiCoMn@N,Co-rGO composite.

Graphene oxide was synthesized using an improved Hummers' method. Briefly, graphite powder was mixed with sulfuric acid and phosphoric acid and stirred for 24 hours. Potassium permanganate was gradually introduced, followed by stirring the mixture at 40 °C for 6 hours. Following this, hydrogen peroxide was introduced, and the reaction proceeded at 50 °C for an additional 3 hours. The obtained suspension was centrifuged, extensively washed with HCl and DI water until reaching a neutral pH, and finally freeze-dried for 24 hours. Cobalt- and nitrogen-doped reduced graphene oxide (N,Co-rGO) was prepared through dispersing graphene oxide in water, followed by sonication. Cobalt chloride solution was then added, and

the mixture was further sonicated before freeze-drying. The resulting powder was thermally treated at 750 °C under argon and ammonia to produce N,Co-rGO.

The Co-Ni-Mn oxides were synthesized through the co-precipitation of metal ions from their nitrate salts, followed by thermal decomposition (calcination) under limited air conditions in a muffle furnace. A solution containing cobalt nitrate hexahydrate, nickel nitrate hexahydrate, and manganese nitrate tetrahydrate in a molar ratio of 2:1:1 was prepared by dissolving the salts in DI water, followed by adjusting the pH of the solution to 9.5 by gradual addition of an alkaline solution (mixture of NaOH and Na_2CO_3) with intense stirring. The resulting suspension was aged at 40 °C with continuous magnetic stirring for 24 hours to ensure complete precipitation. The brown precipitate was separated via centrifugation, thoroughly washed several times with DI water, and and subsequently dried under vacuum. This precursor was then subjected to calcination in air at 500 °C for 4 hours, leading to the formation of Co-Ni-Mn oxides.

The NiCoMn@N,Co-rGO composite was prepared using a hydrothermal method. Initially, N,Co-rGO was dispersed in ethanol and subjected to sonication to form a homogeneous suspension. The as-synthesized Co-Ni-Mn oxides sample was added into the suspension with intense stirring. Subsequently, 10 mL of 6% ammonia solution was gradually added dropwise to the mixture. The mixture was then refluxed in 80 °C for 10 hours, before being transferred to a Teflon-lined autoclave for hydrothermal treatment at 150 °C for 3 hours. Following the reaction, the product was thoroughly washed with deionized water and ethanol, followed by drying in a vacuum oven at 60 °C. During the hydrothermal process, residual functional groups on the N,Co-rGO surface were reduced, and the NiCoMn oxide particles were uniformly embedded onto the graphene matrix. Ammonia served both as a reducing agent and a nitrogen source, further enhancing the composite's structural and electrochemical properties.

2.2. Characterization

In this study, the synthesized catalysts were characterized from both physiochemical and electrochemical perspectives. The physiochemical characterization included a variety of analyses, such as FTIR, XRD, Raman spectroscopy, FESEM and TEM. These methods were employed to thoroughly examine the structural and compositional characteristics of the catalysts. The electrochemical evaluation focused on two key reactions in water electrolysis: the hydrogen and oxygen evolution reactions (HER and OER).

For the physiochemical analysis, the crystalline structure and phase composition of the nanostructured catalysts were first analyzed using X-ray diffraction (XRD) with a Rigaku Ultima IV device. The diffraction profiles were recorded over a 2θ range from 10° to 80°. To examine the surface morphology, field emission scanning electron microscopy (FESEM) was conducted on a TESCAN Mira3 microscope. Transmission electron microscopy (TEM) images were captured with a Philips EM 208S TEM at an accelerating voltage of 100 kV, to observe

the internal structure and particle size distribution of the catalysts. Raman spectroscopy was conducted with a Renishaw 2000 Raman microscope. Fourier transform infrared (FTIR) spectra were obtained using a Bruker Tensor27 spectrometer in the 4000–450 cm^{-1} range to investigate the functional groups present in the catalysts.

On the electrochemical side, the performance of the catalysts for the HER and OER reactions was evaluated using electrochemical techniques. Linear sweep voltammetry (LSV) was employed to assess the catalytic activity, study reaction kinetics, and determine the overpotential. The electrochemical assessments were conducted using a three-electrode system comprising a working, reference, and counter electrode, connected to a potentiostat (Autolab PGSTAT204). The glassy carbon electrode, coated with the catalyst ink, served as the working electrode. An Ag/AgCl electrode immersed in a KCl solution was employed as the reference electrode to provide a stable and reproducible reference potential. A graphite rod was utilised as the counter electrode to complete the electrochemical circuit and facilitate current flow during the experiments. The catalyst ink was prepared by dispersing 2 mg of the synthesized catalyst in a solvent mixture consisting of 0.5 mL DI water and 0.5 mL ethanol. To improve the stability and adhesion of the ink on the electrode surface, 10 µL of Nafion solution was added to the dispersion. Nafion serves as a critical component in preparing catalyst ink for three-electrode voltammetry by functioning as a binder that secures catalyst particles to the working electrode, ensuring a stable and uniform film. It also facilitates proton conductivity, enhancing ionic transport between the catalyst and the electrolyte, which is essential for reactions like HER and OER. Additionally, Nafion improves electrical connectivity by minimizing contact resistance, helps prevent catalyst detachment during electrochemical testing, and provides chemical stability under various electrochemical conditions, ensuring reliable and reproducible measurements.

The mixture was then subjected to ultrasonication to ensure a homogeneous suspension, providing a uniform catalyst distribution for subsequent electrochemical analyses. Subsequently, 6 µL of the catalyst ink was deposited onto the surface of a glassy carbon electrode (2 mm radius) and dried under infrared light to ensure uniform film formation. This prepared electrode was then employed as the working electrode for subsequent electrochemical measurements.

The electrochemical analyses for the hydrogen evolution reaction and oxygen evolution reaction were carried out under controlled conditions to ensure accuracy and reproducibility. For the HER analysis, the experiments were performed in a 0.5 M H_2SO_4 (sulfuric acid) electrolyte, which was saturated with nitrogen (N_2) gas. Nitrogen saturation was employed to remove dissolved oxygen from the solution, thereby preventing any interference from oxygen related reactions that could affect the accuracy of HER measurements. In the case of the OER analysis, the experiments were conducted in a 1 M KOH (potassium hydroxide) solution with a pH of 14, saturated with oxygen (O_2) gas. Oxygen saturation ensures equilibrium between

the electrolyte and the surrounding atmosphere, minimizing oxygen depletion during the OER process and maintaining consistent reaction kinetics.

The Linear Sweep Voltammetry (LSV) technique was used to evaluate the catalytic activity for both HER and OER. For the OER test, the potential range was scanned from 0 V to 1 V vs. Ag/AgCl. This range was selected to encompass the region where the OER typically occurs, allowing for the determination of overpotential and catalytic performance at various current densities. For the HER test, the LSV potential range was set from -1.2 V to -0.2 V vs. Ag/AgCl. This range includes the region where hydrogen evolution becomes significant, enabling the assessment of catalyst efficiency and kinetic parameters.

In this study, all potentials recorded against Ag/AgCl electrode were converted to potentials for Reversible Hydrogen Electrode (RHE) potentials, using the equation: $V_{RHE} = V_{Ag/AgCl}+0.059\times pH+0.197$. The pH values for the electrolytes were 14 for 1 M KOH and 0.3 for 0.5 M H_2SO_4.

3. RESULTS AND DISCUSSION

In this study, the synthesized nanocomposite, NiCoMn@N,Co-rGO, was systematically investigated through two key approaches: physicochemical characterization and electrochemical analysis. The physicochemical characterization was conducted using various techniques, including FESEM, TEM, Raman spectroscopy, FTIR, and XRD. For the electrochemical analysis, voltammetry method was used.

The morphology of the synthesized materials was analyzed using advanced electron microscopy techniques, including field emission scanning electron microscopy (FESEM) and transmission electron microscopy (TEM), as discussed in the previous section. Figure 1 (a) displays the FESEM images of the NiCoMn oxide catalyst, revealing a heterogeneous particle size distribution. This variability in particle size can be ascribed to the presence of a mixture of metal oxides, including nickel (Ni), cobalt (Co), and manganese (Mn) oxides, as well as possible binary oxide phases such as MnCo and NiCo oxides. The diversity in particle composition and size highlights the complexity of the synthesized material's structure.

In contrast, Figure 2 (b-d) presents the FESEM images of the NiCoMn@N,Co-rGO catalyst, showing a distinct structural arrangement. In this composite, the metal oxide particles appear to be encapsulated by reduced graphene oxide (rGO) sheets. This embedding results in a more desirable carbon-metal oxide configuration, where the rGO sheets not only provide a conductive matrix but also stabilize the metal oxide particles, preventing agglomeration. Such a configuration is beneficial for enhancing the material's electrocatalytic performance, as the rGO sheets improve charge transfer efficiency while maintaining structural integrity. This hybrid morphology is crucial for applications in electrochemical processes, as it combines the catalytic activity of the metal oxides with the electrical conductivity and mechanical strength of the rGO support.

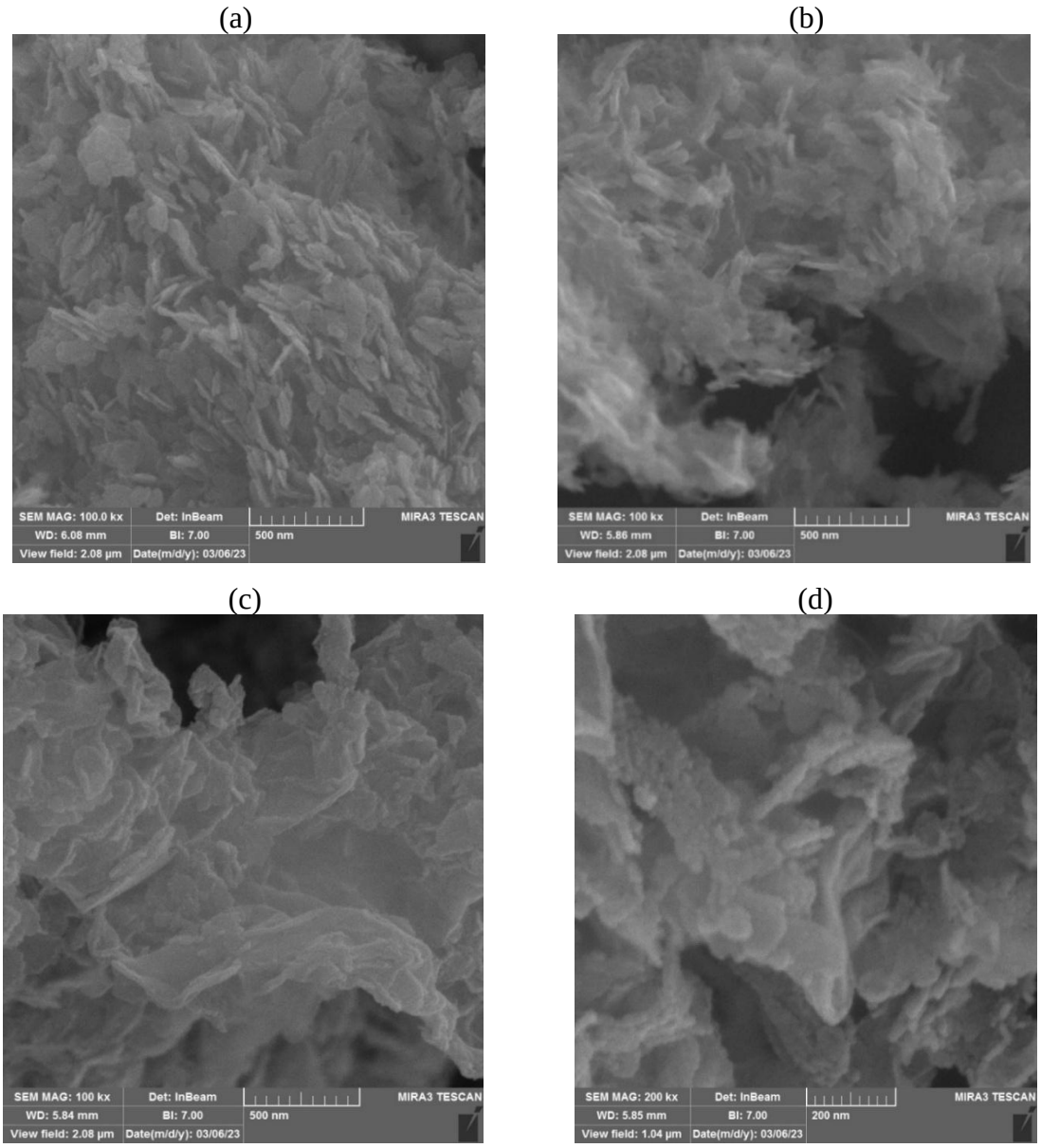

Figure 1. The FESEM images of (a) the NiCoMn oxide, (b-d) the NiCoMn@N,Co-rGO

Figure 2 shows the TEM images of the NiCoMn@N,Co-rGO composite. The micrograph reveals a hierarchical structure with dispersed dark contrast regions, likely corresponding to NiCoMn oxide nanoparticles, embedded within a lighter, sheet-like matrix, which is typical of reduced graphene oxide (rGO). The nanoparticles appear to aggregate to some extent but remain distributed over the graphene surface. The dark particles (NiCoMn oxides) are in the nanometer range, with some appearing below 50 nm in diameter. This nanoscale size facilitates enhanced surface area, which is crucial for catalytic activity in reactions like HER or OER. The lighter areas exhibit a characteristic thin, sheet-like morphology of reduced graphene oxide, which serves as a conductive support material.

The graphene framework appears partially wrinkled or folded, which could enhance the overall mechanical stability and provide sites for embedding nanoparticles. The close interaction between the NiCoMn oxides and the rGO matrix suggests strong adhesion, possibly due to doping with nitrogen and cobalt. This interaction can improve electron transfer efficiency during electrochemical processes. This TEM image highlights the successful synthesis of a hybrid material consisting of NiCoMn oxides embedded on N,Co-doped reduced graphene oxide. The observed structural features, such as the nanoscale dispersion of oxides, the wrinkled graphene sheet morphology, and the interaction between the components, indicate that the material is well-suited for electrocatalytic applications, particularly in HER and OER. However, controlling nanoparticle aggregation and improving the uniformity of dispersion may further enhance its performance.

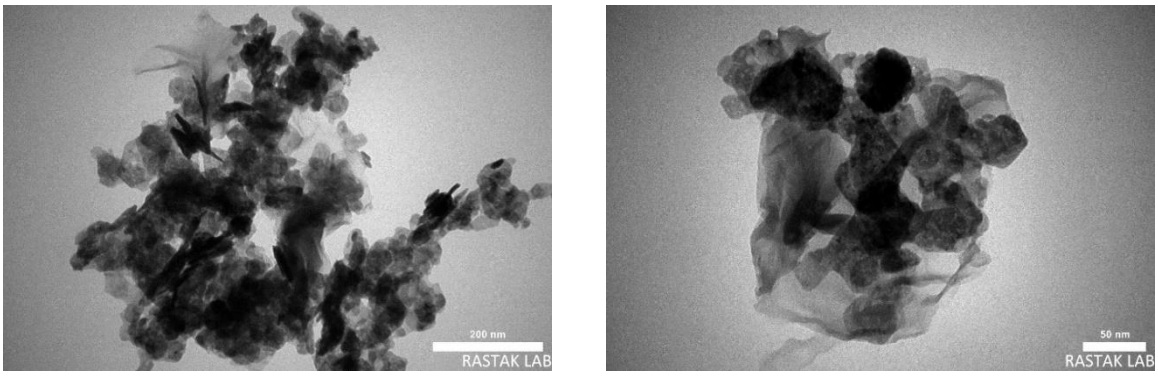

Figure 2. The TEM images of the NiCoMn@N,Co-rGO

Figure 3 presents the FTIR spectra of the NiCoMn oxides sample and the NiCoMn@N,Co-rGO composite, highlighting the presence of distinctive functional groups and chemical bonds within the structures. The FTIR analysis of the NiCoMn@N,Co-rGO composite identified various functional groups, including O-H stretching and bending vibrations at 3430 cm^{-1} and 1640 cm^{-1}, C-O at 1185 cm^{-1}, and C=O at 1727 cm^{-1}. Additionally, signals corresponding to aromatic sp^2 C=C bonds (1621 cm^{-1}), symmetric and asymmetric $–CH_2$ stretching vibrations (2862 and 2935 cm^{-1}, associated with C-H stretching), and N-H stretching (3450 cm^{-1}) were observed. Peaks indicative of C=N, N=O, C-N, and C-OH bonds, were also detected, at wavenumbers of 1640, 1482, 1556 and 1400 cm^{-1}, respectively. Furthermore, carbonate ions (CO_3^{2-}) showed absorption at 1350 cm^{-1}, while C-O-C bonds were evident at 1094 cm^{-1}. Vibrational modes below 1000 cm^{-1} were attributed to overlapping metal oxides and metal hydroxide bonds.

Additionally, the presence of a distinct C=C peak, accompanied by the pair peaks at 2862 cm^{-1} and 2935 cm^{-1} corresponding to symmetric and asymmetric stretching vibrations of $–CH_2$ groups, suggests the re-establishment of the carbon basal plane within NiCoMn@N,Co-rGO composite. The reconstructed carbon basal plane significantly enhances the electrocatalytic

efficiency of the materials by offering an extensive surface area to support NiCoMn oxides as a catalyst for OER and HER.

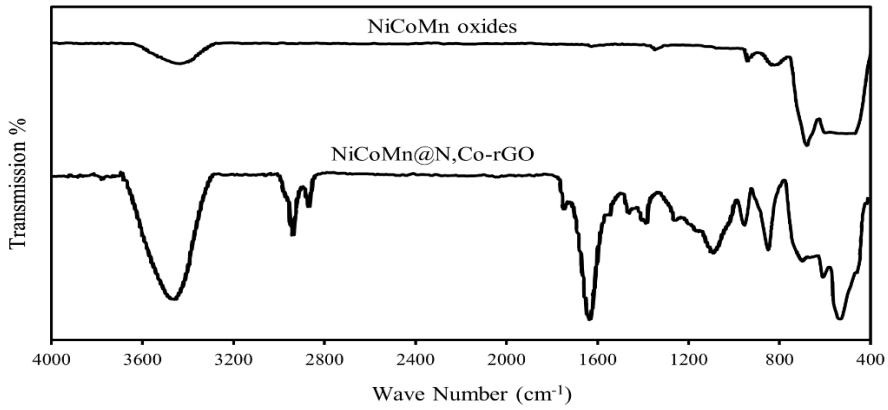

Figure 3. The FTIR spectra of the NiCoMn oxides sample and the NiCoMn@N,Co-rGO composite

Figure 4 presents the XRD patterns of the synthesized catalysts, providing insights into their crystalline structures. The XRD analysis revealed several distinct peaks for the NiCoMn oxides sample, corresponding to various metal oxides such as NiO, MnO, MnO_2, Mn_2O_3, and Co_3O_4, along with binary oxides like $NiCo_2O_4$ and $MnCo_2O_4$ [3,16–23].

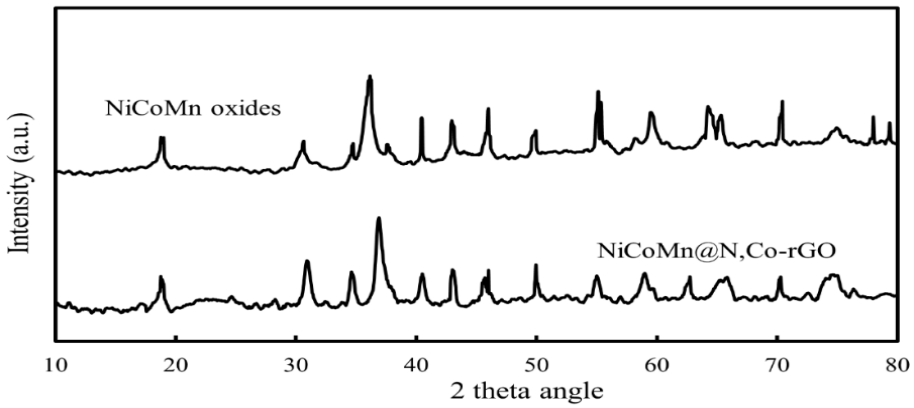

Figure 4. The XRD patterns of the NiCoMn oxides and the NiCoMn@N,Co-rGO composite

These peaks indicate the coexistence of multiple crystalline phases, reflecting the complex composition of the sample. In contrast, the XRD pattern of the NiCoMn@N,Co-rGO composite exhibits a noticeable difference. A newly emerged broad peak appears centered at approximately $2\theta \approx 24°$ emerges, which is absent in the NiCoMn oxides sample. This peak is due to the presence of reduced graphene oxide (rGO), signifying the successful integration of rGO into the composite. The broad nature of this peak suggests the disordered stacking or

partially reduced nature of graphene layers, which is characteristic of rGO. This structural feature enhances the composite's properties by improving electrical conductivity and providing a robust support framework for the metal oxides.

Figure 5 presents the Raman spectra of NiCoMn oxides and the NiCoMn@N,Co-rGO composite. Raman spectroscopy serves as a valuable technique for analyzing carbon-based composites, providing insights into structural irregularities and internal disorder in the material. The Raman spectrum of NiCoMn@N,Co-rGO exhibits prominent D (~1350 cm^{-1}) and G (~1580 cm^{-1}) bands, characteristic of reduced graphene oxide (rGO). The D-band signifies the presence of structural defects, likely introduced by nitrogen and doping and the embedding of NiCoMn oxides, while the G-band corresponds to the in-plane vibrations of sp^2-hybridized carbon, indicating preserved graphitic domains. The intensity ratio (I_D/I_G) indicates the level of disorder in the rGO lattice. A moderate I_D/I_G ratio, as observed here, suggests an optimal balance between defects and graphitic order, critical for enhancing catalytic activity and maintaining conductivity. The spectrum reveals that the material combines defect-rich regions for catalytic activity with sufficient graphitization to ensure effective electron transport. The structural balance attained through doping and functionalization positions NiCoMn@N,Co-rGO as a promising candidate for catalytic applications in water electrolysis processes. The broad peak observed below 700 cm^{-1} in the Raman spectrum is attributed to the superposition of multiple peaks corresponding to various metal oxide species.

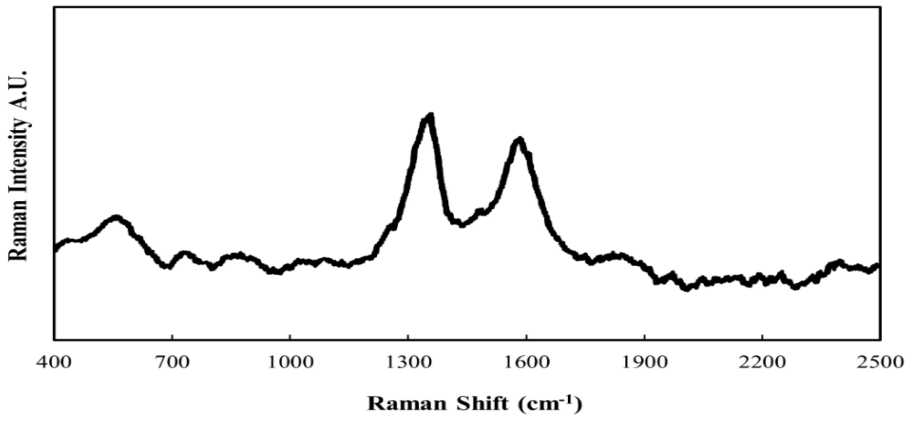

Figure 5. The Raman Spectra of NiCoMn oxides and the NiCoMn@N,Co-rGO composite

For electrochemical evaluation, Figure 6 presents the OER and HER performance characterization plots, including linear sweep voltammetry (LSV), and overpotential for the synthesized NiCoMn oxides and NiCoMn@N,Co-rGO catalysts in a 1 M KOH solution and 0.5 M H_2SO_4. It is worth to note that the all the potential values were measured versus Ag/AgCl electrode and converted to RHE.

The LSV analysis for the OER demonstrates that the NiCoMn@N,Co-rGO composite achieves a potential of 1.58 V at a current density of 10 mA/cm^2, corresponding to an

overpotential of 0.27 V. In contrast, the NiCoMn oxide requires a higher potential of 1.62 V to reach the same current density, resulting in an overpotential of 0.50 V. For the HER, the LSV analysis shows that the NiCoMn@N,Co-rGO composite reaches a potential of -0.50 V at a current density of -10 mA/cm², corresponding to an overpotential of 0.49 V, whereas the NiCoMn oxide achieves a potential of -0.49 V vs RHE at the same current density.

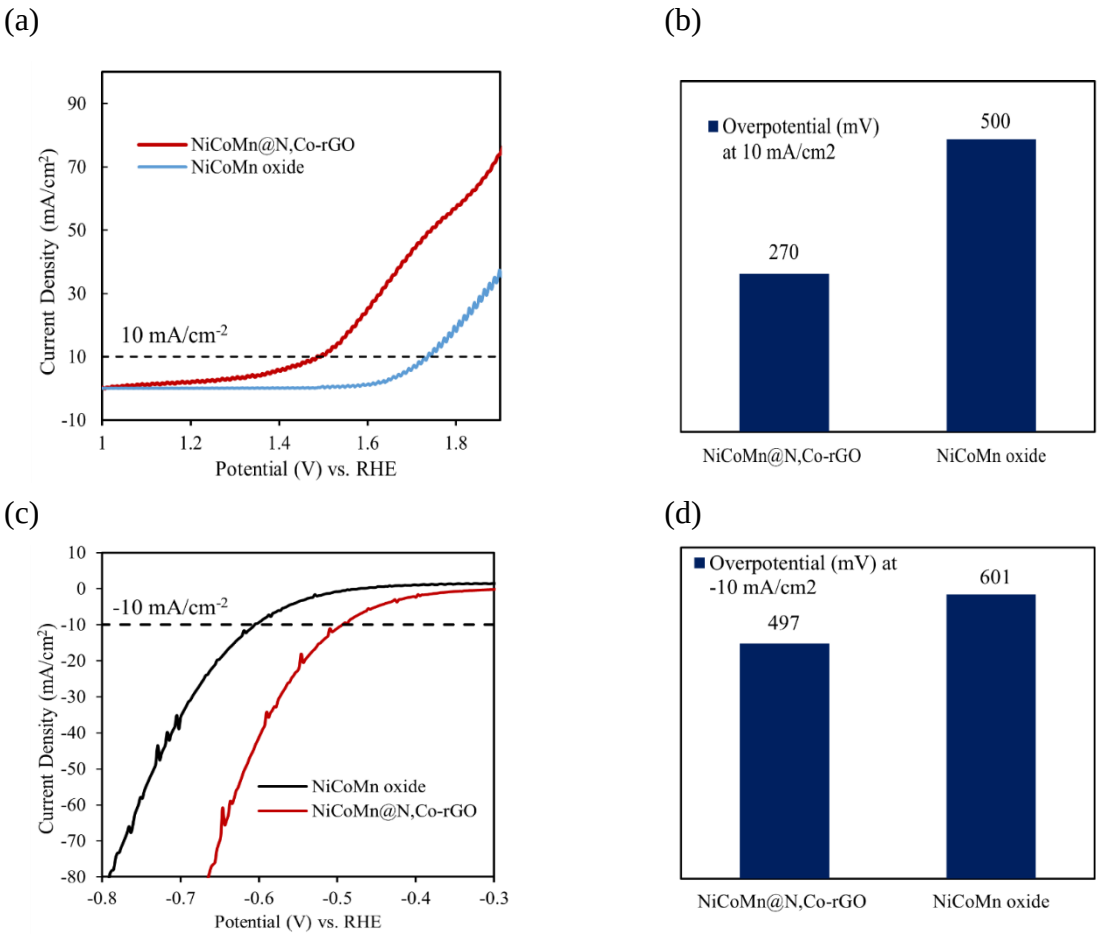

Figure 6. (a), (c) The Linear Sweep Voltammetry of the NiCoMn oxide sample and NiCoMn@N,Co-rGO, for OER and HER; (b), (d) the overpotential of the synthesized samples at current densities of 10 mA/cm2 for OER and -10 mA/cm2 for HER

The reduced overpotential of the NiCoMn@N,Co-rGO composite highlights its superior catalytic activity for the oxygen evolution reaction in alkaline media and its acceptable performance for the hydrogen evolution reaction. This enhanced performance is ascribed to the synergistic effects of nitrogen and cobalt doping within the reduced graphene oxide framework, which improve electrical conductivity, active site accessibility, and structural stability. These results establish the NiCoMn@N,Co-rGO composite as a more efficient electrocatalyst for OER compared to NiCoMn oxide.

4. CONCLUSION

In this study, the NiCoMn@N,Co-rGO composite was synthesized and systematically characterized for its electrocatalytic performance in water electrolysis. Physicochemical analysis confirmed the successful integration of Co-Ni-Mn oxides into a nitrogen and cobalt-doped reduced graphene oxide (rGO) framework. Electrochemical evaluation revealed superior catalytic activity for the Oxygen Evolution Reaction (OER), achieving an overpotential of 0.27 V at 10 mA/cm², meaningfully lower than the 0.50 V obtained for NiCoMn oxides. For the Hydrogen Evolution Reaction (HER), the composite demonstrated an overpotential of 0.49 V at -10 mA/cm², indicating acceptable performance. The synergistic effects of nitrogen and cobalt doping in the rGO framework are attributed to these enhancements, making NiCoMn@N,Co-rGO a promising electrocatalyst for efficient water electrolysis, particularly for OER in alkaline media. Our findings advance the development of efficient and cost-effective electrocatalysts for water splitting, contributing to the broader goal of sustainable hydrogen production. The promising performance of the NiCoMn@N,Co-rGO composite in HER and OER catalysis highlights the potential of doped carbon-based materials for energy conversion applications. Future research could explore the incorporation of other transition metals or alloy systems onto doped graphene frameworks to further enhance catalytic activity and durability under diverse operating conditions.

Acknowledgments

This work is based upon research funded by Iran National Science Foundation - Project No. 4028557.

Declarations of interest

The authors declare no conflict of interest in this reported work.

REFERENCES

[1] M. Aghbashlo, M. Tabatabaei, S.S. Hosseini, H. Younesi, and G. Najafpour, Clean Technol. Envir. 18 (2016) 853.

[2] S.S. Hosseini, M. Mehrpooya, and M.H. Jahangir, Anal. Bioanal. Electrochem. 15 (2023) 1098.

[3] S.S. Hosseini, M. Mehrpouya, and M.H. Jahangir, Mater. Chem. Phys. 314 (2024) 128838.

[4] P. Hu, F.F. Yang, F. Yang, F. Zhu, J. Luo, X. Chen, W. Li, J. Bian, L. Gao, K. Wang, and Z. Yin, J. Colloid Interface Sci. 680 (2025) 427.

[5] M. Mehrpooya, M. Hadavand, and M.R. Ganjali, Mater. Chem. Phys. (2024) 130076.

[6] C. He, and J. Tao, Int. J. Hydrogen Energy 47 (2022) 13240.

[7] Y. Zhang, Y. Yang, B. Lu, R.R. Zhang, F. Zhou, Q. Wang, J. Li, Z. Yang, and Z. Lei, J. Alloys Compd. 1006 (2024) 176310.
[8] R. Zhang, Q. Liu, L. Zhou, L. Wang, L. Cheng, A. Xie, H. Xu, Z. Bai, Y. Tang, and P. Wan, Int. J. Hydrogen Energy 82 (2024) 1341.
[9] A. Soni, S. Kumar Maurya, M. Malviya, D. Tiwary, J. Electroanal. Chem. 972 (2024) 118640.
[10] Z. Qin, W. Liu, W. Que, J. Feng, W. Shi, F. Wu, and X. Cao, ChemPhysMater 2 (2023) 185.
[11] B. Tamilarasi, K.P. Jithul, and J. Pandey, Int. J. Hydrogen Energy 58 (2024) 556.
[12] Z.G. Yang, H.M. Xu, T.Y. Shuai, Q.N. Zhan, Z.J. Zhang, K. Huang, C. Dai, and G.R. Li, Nanoscale 15 (2023) 11777.
[13] T. Lagarteira, S. Delgado, G.P. Garcia, A. Ortiz, and A. Mendes, Int. J. Hydrogen Energy 48 (2023) 20901.
[14] L. Hong, Z. Liu, X. Zhang, Y. Xue, H. Huang, Q. Jiang, and J. Tang, J. Alloys Compd. 991 (2024) 174238.
[15] B. Yang, Y. Jin, L. Tian, X. Liu, M. Liu, W. Xiao, X. Wu, J. Ge, Y. Li, A. Aierken, G. Wang, D. Wang, Z. Wang, Y. Wu, W. Deng, C. Gao, and J. Bi, Surfaces and Interfaces (2024) 105532.
[16] D. Wang, X. Chen, D.G. Evans, and W. Yang, Nanoscale 5 (2013) 5312.
[17] R. Nie, J. Shi, W. Du, W. Ning, Z. Hou, and F.S. Xiao, J. Mater. Chem. A Mater. 1 (2013) 9037.
[18] N. Mironova-Ulmane, A. Kuzmin, V. Skvortsova, G. Chikvaidze, I. Sildos, J. Grabis, D. Jankoviča, A. Dindune, and M. Maiorov, Acta Phys Pol A 133 (2018) 1013.
[19] S.L. Kadam, S.M. Mane, P.M. Tirmali, and S.B. Kulkarni, Current Applied Physics 18 (2018) 397.
[20] L. Zhang, D. Ge, H. Geng, J. Zheng, X. Cao, and H. Gu, New J. Chem. 41 (2017) 7102.
[21] M. Wu, S. Meng, Q. Wang, W. Si, W. Huang, and X. Dong, ACS Appl. Mater. Interfaces 7 (2015) 21089.
[22] X. Rong, F. Qiu, J. Qin, H. Zhao, J. Yan, D. Yang, J. Industrial Eng. Chem. 26 (2015) 354.
[23] Y.J. Mai, S.J. Shi, D. Zhang, Y. Lu, C.D. Gu, and J.P. Tu, J Power Sources 204 (2012) 155.